

Heralded magnetism in non-Hermitian atomic systems

Tony E. Lee and Ching-Kit Chan

*ITAMP, Harvard-Smithsonian Center for Astrophysics, Cambridge, MA 02138, USA and
Department of Physics, Harvard University, Cambridge, MA 02138, USA*

(Dated: February 28, 2014)

We study the non-equilibrium phase transitions of the non-Hermitian XY model, which can be implemented with cold atoms. The non-Hermitian model is heralded by the absence of a decay event. We exactly solve the one-dimensional model using the Jordan-Wigner transformation. The phase diagram is entirely different from those of the Hermitian model and the master equation. There is a quantum phase transition from short-range order to quasi-long-range order despite the lack of a continuous symmetry. The critical exponent ν can be 1 or 1/2. The ordered phase has a non-classical, non-repeating spin pattern. Our results can be seen experimentally with trapped ions, cavity QED, and atoms in optical lattices.

Introduction.— A goal of condensed matter physics is to find new phases and phase transitions. A driving force behind cold-atom research is the ability to implement new condensed-matter models that would otherwise be impossible in solid state. In particular, cold atoms provide the opportunity to study nonequilibrium phases, since dissipation arises naturally from spontaneous emission [1]. In this case, the phases are nonequilibrium steady states instead of equilibrium ground states. Recent works have shown that dissipation can qualitatively change phase diagrams and even create new, exotic phases without an equilibrium counterpart [2–20]. These works have been based on the master-equation framework, which assumes that when an atom decays, the population remains in the Hilbert space.

In this paper, we study the nonequilibrium phases due to a different type of dissipation: we consider the steady state of a non-Hermitian Hamiltonian instead of a master equation. Suppose each atom has states $|\uparrow\rangle$ and $|\downarrow\rangle$, but $|\uparrow\rangle$ decays into an auxiliary state $|a\rangle$ instead of $|\downarrow\rangle$ [Fig. 1(a)]. Then, conditioned on the absence of a decay event, $|\uparrow\rangle$ and $|\downarrow\rangle$ evolve according to a non-Hermitian Hamiltonian [1, 21, 22]. Thus, the non-Hermitian evolution is “heralded” by the absence of population in $|a\rangle$. This is similar to heralded entanglement protocols: a measurement signals the preparation of the desired state without destroying it [23–27].

We consider a one-dimensional chain of atoms that interact according to the anisotropic XY Hamiltonian but with the dissipation described above. After sufficient time, the non-Hermitian evolution prepares the system in a steady-state wavefunction. We show that the steady state exhibits a quantum phase transition from short-range order to quasi-long-range order, which is surprising due to the absence of a continuous symmetry in the Hamiltonian. The critical exponent ν can be either 1 or 1/2, the latter value being unusual for a spin chain. The ordered phase has a non-classical, non-repeating spin pattern not found in either the Hermitian model or the master equation. The phase boundaries are also completely modified. Our results can be experimentally observed in a variety of cold-atom setups, and we provide realistic experimental numbers.

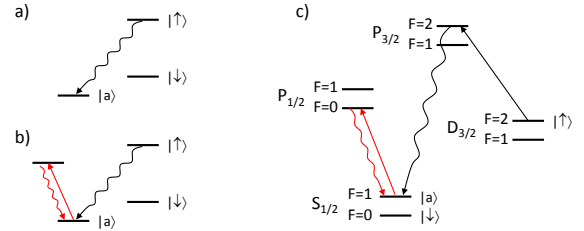


FIG. 1. (a) $|\uparrow\rangle$ decays into the auxiliary state $|a\rangle$. (b) The population of $|a\rangle$ is measured by exciting it with a laser and detecting the fluorescence (red arrows). (c) Level scheme for an $^{171}\text{Yb}^+$ ion, showing optical pumping (black arrows) and detection (red arrows).

It is worth mentioning that non-Hermitian models are known to exhibit a variety of rich behavior [28–31], such as localization transitions [32], topological transitions [33], \mathcal{PT} symmetry [34–36], and spatial condensate order [37]. Non-Hermitian models can also provide information about the dynamics of the corresponding Hermitian model [38]. In this paper, we show how non-Hermitian quantum mechanics leads to new magnetic behavior that can be observed in current cold-atom setups.

Model.— Consider the anisotropic XY model in one dimension with nearest neighbor interactions [39–41]:

$$H = \sum_n (J_x \sigma_n^x \sigma_{n+1}^x + J_y \sigma_n^y \sigma_{n+1}^y). \quad (1)$$

Each atom has states $|\uparrow\rangle$ and $|\downarrow\rangle$, which constitute the relevant Hilbert space, and $\sigma_n^x, \sigma_n^y, \sigma_n^z$ are the Pauli matrices for atom n . We assume that $|\uparrow\rangle$ decays into the auxiliary state $|a\rangle$ with rate γ [Fig. 1(a)]. Then in the absence of a decay event, the system evolves with the effective non-Hermitian Hamiltonian [1, 21, 22]:

$$H_{\text{eff}} = H - \frac{i\gamma}{4} \sum_n (\sigma_n^z + 1). \quad (2)$$

This counter-intuitive effect is due to the fact that the atoms are coupled to the environment, and the environment continuously measures whether a photon has been

emitted. Even when no atom has decayed to $|a\rangle$, the null measurement of photons still affects the wavefunction of the atoms. This measurement back-action is accounted for by the non-Hermitian term in Eq. (2), which transfers population from $|\uparrow\rangle$ to $|\downarrow\rangle$ in a non-unitary way.

The eigenvalues of H_{eff} are complex and have negative imaginary parts [42]. When an initial many-body wavefunction is evolved using $\exp(-iH_{\text{eff}}t)$, the imaginary parts of the eigenvalues cause the weight in each eigenstate to decrease over time, corresponding to leakage of population out of the Hilbert space. However, the eigenvalue with the largest (least negative) imaginary part decays the slowest, so after a sufficient amount of time, the wavefunction consists mostly of the corresponding eigenstate. We call this surviving eigenstate the steady-state wavefunction, and we study its phase diagram.

The experimental protocol is as follows. In each experimental run, the atoms interact via Eq. (1) while possibly decaying into $|a\rangle$. One measures the population in $|a\rangle$ to check whether any atom has decayed [Fig. 1(b)]. This measurement can be done either at the end of the run or continuously during the run. The experimental runs without decay events evolve solely with H_{eff} and thus simulate the model of interest. This scheme is similar to heralded entanglement generation: when a trial succeeds, it is heralded by a measurement outcome [23–27]. Importantly, the heralding does not itself destroy the state. Thus, the magnetic model we study is heralded by the absence of population in $|a\rangle$.

We emphasize that our model is different from the typical dissipative model described by a master equation for the density matrix ρ ,

$$\dot{\rho} = -i[H, \rho] + \gamma \sum_n \left[\sigma_n^- \rho \sigma_n^+ - \frac{1}{2}(\sigma_n^+ \sigma_n^- \rho + \rho \sigma_n^+ \sigma_n^-) \right]. \quad (3)$$

This master equation applies when $|\uparrow\rangle$ decays into $|\downarrow\rangle$ and was discussed previously in Refs. [16, 17]. Below, we show that the phase diagram of H_{eff} is quite different from those of the master equation as well as H . We also emphasize that our model is different from the spin-boson model [43]: we study the nonequilibrium steady state of the system, instead of the equilibrium ground state of the system and environment.

For convenience, we rewrite H_{eff} as

$$H_{\text{eff}} = \sum_n \left[2J(\sigma_n^+ \sigma_{n+1}^- + \sigma_n^- \sigma_{n+1}^+) + 2J'(\sigma_n^+ \sigma_{n+1}^+ + \sigma_n^- \sigma_{n+1}^-) - \frac{i\gamma}{4}(\sigma_n^z + 1) \right], \quad (4)$$

where $J = (J_x + J_y)/2$ and $J' = (J_x - J_y)/2$. There is competition between the non-Hermitian term (measured by γ) and the anisotropic interaction (measured by J') that coherently excites pairs of atoms. This competition leads to the critical behavior discussed below.

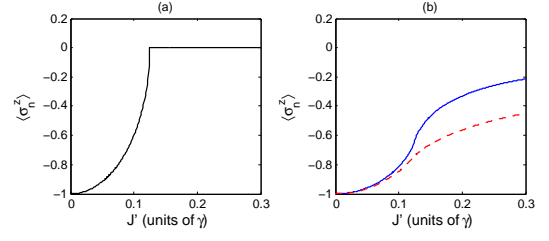


FIG. 2. $\langle \sigma_n^z \rangle$ for (a) two atoms and (b) infinite chain with $J = 0$ (blue solid line) and $J = 0.1\gamma$ (red dashed line). The critical point is $J' = \gamma/8$ for all cases. Panel (a) is independent of J .

Two atoms.— We first consider the case of two atoms, since it is the easiest to realize experimentally. (We assume periodic boundary conditions to match up with the results for larger chains.) H_{eff} has four eigenvalues: $\lambda_1^\pm = -i\gamma/2 \pm (1/2)\sqrt{64J'^2 - \gamma^2}$ and $\lambda_2^\pm = -i\gamma/2 \pm 4J$. When $|J'| < \gamma/8$, λ_1^+ has the largest imaginary part, so there is a single steady state, given by the corresponding eigenstate. When $|J'| \geq \gamma/8$, all four eigenvalues have the same imaginary part, so there is no longer a unique steady state.

A degeneracy occurs when $|J'| = \gamma/8$ since $\lambda_1^+ = \lambda_1^-$ there. This type of non-Hermitian degeneracy is known as an exceptional point [28–30], and the eigenstates exhibit nonanalytic behavior as $|J'|$ passes through $\gamma/8$. The nonanalyticity is most easily seen in $\langle \sigma_n^z \rangle$ [Fig. 2(a)]: when $|J'| < \gamma/8$, the unique steady state has $\langle \sigma_n^z \rangle = -\sqrt{1 - 64(J'/\gamma)^2}$, while when $|J'| \geq \gamma/8$, all four eigenstates have $\langle \sigma_n^z \rangle = 0$. The ability to have critical behavior in finite systems is a unique feature of non-Hermitian Hamiltonians [28–30]. In contrast, finite Hermitian Hamiltonians exhibit avoided crossings.

Note that the steady state is just the eigenstate with the smallest $\langle \sigma_n^z \rangle$. This is because the smaller $\langle \sigma_n^z \rangle$ is, the smaller the probability that an atom decays into $|a\rangle$. The null measurement of photons by the environment projects the system into the eigenstate least likely to emit a photon.

Long chain.— Although two atoms already exhibit nonanalytic behavior, in order to discuss phases and phase transitions, we have to consider a long chain of N atoms. We solve this exactly using the Jordan-Wigner transformation, which maps the interacting model to a model of free fermions [39–41]. Although this is a standard technique for Hermitian systems, there are important differences due to the non-Hermitian nature. Note that the spectra of other non-Hermitian spin chains were considered in Refs. [32, 35, 36, 38].

We map each spin to a fermion: $|\uparrow\rangle = |1\rangle$ and $|\downarrow\rangle = |0\rangle$. The spin operators are written in terms of fermionic creation and annihilation operators: $\sigma_n^+ = c_n^\dagger \exp(i\pi \sum_{m < n} c_m^\dagger c_m)$ and $\sigma_n^z = 2c_n^\dagger c_n - 1$. After going to Fourier space, $c_n = (e^{-i\pi/4}/\sqrt{N}) \sum_k e^{ikn} \tilde{c}_k$, Eq. (4)

becomes

$$H_{\text{eff}} = \sum_{k>0} \left[\begin{pmatrix} \tilde{c}_k^\dagger & \tilde{c}_{-k} \end{pmatrix} M_k \begin{pmatrix} \tilde{c}_k \\ \tilde{c}_{-k}^\dagger \end{pmatrix} - \frac{i\gamma}{2} \right], \quad (5)$$

$$M_k = \begin{pmatrix} 4J \cos k - i\gamma/2 & -4J' \sin k \\ -4J' \sin k & -(4J \cos k - i\gamma/2) \end{pmatrix}. \quad (6)$$

Let the right eigenvectors of M_k be $(u_k, v_k)^T$ and $(-v_k, u_k)^T$. Then after diagonalizing M_k , we obtain

$$H_{\text{eff}} = \sum_k \left[\epsilon(k) \left(\bar{\eta}_k \eta_k - \frac{1}{2} \right) - \frac{i\gamma}{4} \right] \quad (7)$$

$$\epsilon(k) = \pm \sqrt{(4J \cos k - i\gamma/2)^2 + (4J' \sin k)^2}, \quad (8)$$

in terms of non-Hermitian Bogoliubov quasiparticles,

$$\begin{aligned} \eta_k &= u_k \tilde{c}_k + v_k \tilde{c}_{-k}^\dagger, & \eta_{-k} &= -v_k \tilde{c}_k^\dagger + u_k \tilde{c}_{-k} \\ \bar{\eta}_k &= u_k \tilde{c}_k^\dagger + v_k \tilde{c}_{-k}, & \bar{\eta}_{-k} &= -v_k \tilde{c}_k + u_k \tilde{c}_{-k}^\dagger. \end{aligned} \quad (9)$$

$\bar{\eta}_k$ and η_k obey fermionic statistics: $\{\bar{\eta}_k, \eta_{k'}\} = \delta_{kk'}$ and $\{\eta_k, \eta_{k'}\} = \{\bar{\eta}_k, \bar{\eta}_{k'}\} = 0$. So $\bar{\eta}_k$ and η_k act as fermionic creation and annihilation operators. But $\bar{\eta}_k \neq \eta_k^\dagger$ due to the non-Hermitian nature, as seen from Eq. (9).

Thus, Eq. (7) is a model of free η fermions. We define the vacuum state $|G\rangle$ as the state that satisfies $\eta_k |G\rangle = 0$ for all k . (Note that $\langle G | \bar{\eta}_k \neq 0$.) $|G\rangle$ is an eigenstate of H_{eff} , and the other eigenstates are its fermionic excitations: $\bar{\eta}_{k_1} \bar{\eta}_{k_2} \cdots \bar{\eta}_{k_n} |G\rangle$.

The eigenvalue of $|G\rangle$ is $-\sum_k [\epsilon(k) + i\gamma/2]/2$. For each k , we choose the sign convention in Eq. (8) such that the imaginary part of $\epsilon(k)$ is always negative. This way, $|G\rangle$ is the steady state wavefunction, since all other eigenvalues have smaller (more negative) imaginary parts.

A phase transition of $|G\rangle$ occurs when $\epsilon(k) = 0$ for some k , since then an eigenstate is degenerate with $|G\rangle$. This occurs when $|J'| = \gamma/8$, which is the same as for two atoms. To characterize the phases, we calculate several observables for $|G\rangle$:

$$\langle \sigma_n^z \rangle = \frac{1}{\pi} \int_0^\pi dk \frac{-|u_k|^2 + |v_k|^2}{|u_k|^2 + |v_k|^2}, \quad (10)$$

$$\langle \sigma_m^x \sigma_n^x \rangle = \langle B_m A_{m+1} B_{m+1} \cdots A_{n-1} B_{n-1} A_n \rangle, \quad (11)$$

$$\langle \sigma_m^y \sigma_n^y \rangle = (-1)^{n-m} \langle A_m B_{m+1} A_{m+1} \cdots B_{n-1} A_{n-1} B_n \rangle, \quad (12)$$

$$\langle \sigma_m^z \sigma_n^z \rangle = \langle A_m B_m A_n B_n \rangle, \quad (13)$$

where $A_n = c_n^\dagger + c_n$ and $B_n = c_n^\dagger - c_n$. Note that $\langle \sigma_n^x \rangle = \langle \sigma_n^y \rangle = 0$. Using Wick's theorem, Eqs. (11)–(13) can be written as sums over all possible contractions of operator pairs. The Supplemental Material provides the expressions for the pair contractions, which are different from the Hermitian case [39]. In particular, the non-Hermitian algebra leads to the anomalous correlation $\langle \bar{\eta}_k \eta_k \rangle \neq 0$, while $\langle \eta_k \eta_k \rangle = 0$.

We now describe the phases on both sides of the transition. There are two qualitatively different cases, $J \neq 0$ and $J = 0$, which we consider separately.

Case of $J \neq 0$.—Figure 3(a) shows the spectrum $\text{Im } \epsilon(k)$. When $|J'| < \gamma/8$, $\text{Im } \epsilon(k)$ is always negative,

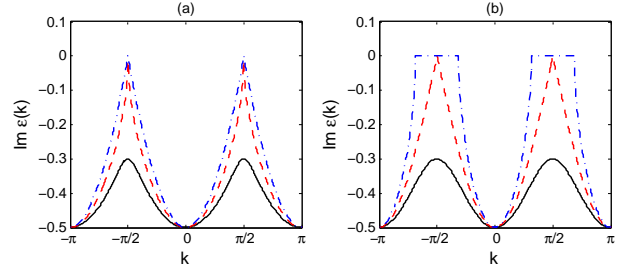


FIG. 3. Imaginary part of spectrum $\epsilon(k)$ for $J' = 0.1\gamma$ (black solid line), $J' = 0.125\gamma$ (red dashed line), and $J' = 0.15\gamma$ (blue dash-dotted line). (a) $J = 0.1\gamma$. (b) $J = 0$.

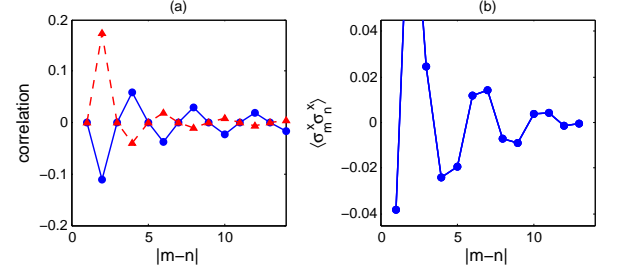


FIG. 4. Correlation functions $\langle \sigma_m^x \sigma_n^x \rangle$ (blue solid line) and $\langle \sigma_m^y \sigma_n^y \rangle$ (red dashed line) for $J' = 0.13\gamma$ with (a) $J = 0.1\gamma$ and (b) $J = 0$.

so $|G\rangle$ is “gapped,” i.e., the imaginary part of its eigenvalue is offset from all other eigenvalues by a nonzero amount. When $|J'| \geq \gamma/8$, $\text{Im } \epsilon(k) = 0$ for $k = \pm\pi/2$, so $|G\rangle$ has gapless excitations.

Figure 4(a) shows the correlation functions for $|G\rangle$. In general, $\langle \sigma_m^x \sigma_n^x \rangle$ and $\langle \sigma_m^y \sigma_n^y \rangle$ are zero for odd distances, which implies that the chain divides into two alternating sublattices with a degree of freedom between them. (However, $\langle \sigma_m^x \sigma_n^y \rangle$ is nonzero only for odd distances.) When $|J'| < \gamma/8$, the correlations $\langle \sigma_m^x \sigma_n^x \rangle$, $\langle \sigma_m^y \sigma_n^y \rangle$, and $\langle \sigma_m^z \sigma_n^z \rangle - \langle \sigma_m^z \rangle \langle \sigma_n^z \rangle$ for even distances decay exponentially with distance. When $|J'| \geq \gamma/8$, they decay according to a power law. So within each sublattice, there is short-range order for $|J'| < \gamma/8$ and quasi-long-range order for $|J'| \geq \gamma/8$ [Fig. 5(a)].

As $|J'|$ increases towards $\gamma/8$, the correlation length ξ diverges as $\sim (\gamma/8 - |J'|)^{-\nu}$ where ν is the critical exponent [Fig. 5(c)]. In the Supplemental Material, we analytically calculate $\langle \sigma_m^z \sigma_n^z \rangle - \langle \sigma_m^z \rangle \langle \sigma_n^z \rangle$ for large distances and show that $\nu = 1$, which is the same as for Hermitian spin models in one dimension [41]. Numerically, we find that $\langle \sigma_m^x \sigma_n^x \rangle$ and $\langle \sigma_m^y \sigma_n^y \rangle$ also have $\nu = 1$. From Eq. (7), we find that the dynamical critical exponent z is $1/2$.

The quasi-long-range order here is quite surprising. In Hermitian systems, quasi-long-range order occurs when the Hamiltonian has a continuous symmetry. However, H_{eff} does not have a continuous symmetry when $J \neq 0$. Also, the ordered state is peculiar in the sense

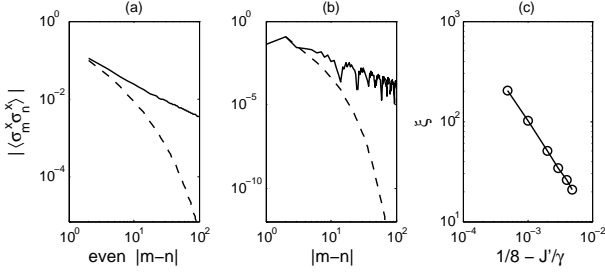


FIG. 5. Correlation functions for $J' = 0.13\gamma$ (solid line) and $J' = 0.12\gamma$ (dashed line) for (a) $J = 0.1\gamma$ and (b) $J = 0$. (c) Correlation length $\xi(J')$ for $J = 0.1\gamma$, found by fitting exponential decay of $\langle\sigma_m^x\sigma_n^x\rangle$. Panel (b) shows only even distances for $J' = 0.12\gamma$. All plots are log-log.

that $\langle\sigma_m^x\sigma_n^x\rangle$ and $\langle\sigma_m^y\sigma_n^y\rangle$ always have opposite signs [Fig. 4(a)]. This implies that the spin pattern within a sublattice does not repeat. For a more familiar state like an antiferromagnet, $\langle\sigma_m^x\sigma_n^x\rangle$ and $\langle\sigma_m^y\sigma_n^y\rangle$ have the same sign at periodic distances. Thus, the ordered state here is non-classical in nature and does not seem to be previously known.

Case of $J = 0$.— Figure 3(b) shows the spectrum $\text{Im } \epsilon(k)$ for this case. When $|J'| < \gamma/8$, the steady state is gapped as before. When $|J'| = \gamma/8$, the gap closes at $k = \pm\pi/2$. But when $|J'| > \gamma/8$, $\text{Im } \epsilon(k) = 0$ for an extended range around $k = \pm\pi/2$, meaning that the steady state is highly degenerate.

Figure 4(b) shows the correlation functions for $\langle G \rangle$. In general, $\langle\sigma_m^x\sigma_n^x\rangle = \langle\sigma_m^y\sigma_n^y\rangle$. When $|J'| < \gamma/8$, $\langle\sigma_m^x\sigma_n^x\rangle$, $\langle\sigma_m^y\sigma_n^y\rangle$, and $\langle\sigma_m^z\sigma_n^z\rangle - \langle\sigma_m^z\rangle\langle\sigma_n^z\rangle$ are zero for odd distances, and their values for even distances decay exponentially in distance. But when $|J'| \geq \gamma/8$, they are nonzero for all distances and form a spin-density-wave pattern, whose magnitude decays according to a power law [Fig. 5(b)].

In the Supplemental Material, we show analytically that the correlation length ξ diverges with critical exponent $\nu = 1/2$. It is surprising that this is not 1, which is the value for $J \neq 0$ as well as for Hermitian spin chains. The dynamical critical exponent z is 1.

Figure 2(b) plots $\langle\sigma_n^z\rangle$. When $|J'| \leq \gamma/8$, $\langle\sigma_n^z\rangle = -\frac{2}{\pi}E(64J'^2)$, where $E(x)$ is the complete elliptic integral of the second kind. Interestingly, $d\langle\sigma_n^z\rangle/dJ'$ exhibits a logarithmic divergence at $|J'| = \gamma/8$. (This singularity does not occur when $J \neq 0$.)

Comparison with Hermitian model and master equation.— The ground state of the Hermitian model [Eq. (1)] is either ferromagnetic or anti-ferromagnetic [39]. There is long-range order, except when $|J_x| = |J_y|$, in which case there is quasi-long-range order. If H included a real field $\sum_n (h/4)\sigma_n^z$, then there would be short-range order when $|J| < h/8$ with $\nu = 1$ [40].

The steady-state density matrix of the master equation [Eq. (3)] has only short-range order in one dimension [17]. Mean-field theory predicts that when $J_x J_y > -\gamma^2/64$,

the system is in the staggered-XY phase, characterized by $\langle\sigma_m^x\sigma_n^x\rangle$ and $\langle\sigma_m^y\sigma_n^y\rangle$ being 0 for odd distances and both positive for even distances [16].

The magnetic behavior of the non-Hermitian model is qualitatively different from both the Hermitian model and the master equation. It has a phase transition in one dimension and in fact already exhibits critical behavior for two atoms. There is quasi-long-range order for $|J'| > \gamma/8$, which is an extended area in J_x, J_y space instead of a line as in the Hermitian case. ν can be $1/2$, which is different from the Hermitian case. The ordered phases are also different. Since $\langle\sigma_m^x\sigma_n^x\rangle$ and $\langle\sigma_m^y\sigma_n^y\rangle$ always have opposite signs when $J \neq 0$, the ordered phase is different from both the staggered-XY phase and the antiferromagnetic phase. In addition, the spin-density-wave phase (for $J = 0$) is not present in either the Hermitian model or the master equation.

We emphasize that H_{eff} has different critical behavior than the master equation even though both include dissipation. Recent works indicate that master equations have classical phase transitions because dissipation introduces an effective temperature [3, 4]. Since H_{eff} has a phase transition in one dimension, it is a quantum phase transition [41].

Experimental implementation.— The Hermitian XY-model [Eq. (1)] can be implemented using trapped ions [44–47], an array of cavities [15, 17], atoms within a cavity [13], and Rydberg atoms in optical lattices [16, 48–50]. To implement the non-Hermitian model [Eq. (2)], one would optically pump $|\uparrow\rangle$ into the auxiliary state $|a\rangle$.

We discuss a specific realization using trapped $^{171}\text{Yb}^+$ ions [Fig. 1(c)]. Let $|\downarrow\rangle$ be $|S_{1/2}, F=0\rangle$, let $|\uparrow\rangle$ be $|D_{3/2}, F=2\rangle$, and let $|a\rangle$ be $|S_{1/2}, F=1\rangle$. One would optically pump $|\uparrow\rangle$ to $|P_{3/2}, F=2\rangle$, which decays into $|a\rangle$ instead of $|\downarrow\rangle$ due to dipole selection rules. J and J' can be on the order of $2\pi \times 1$ kHz [47], and one can set $\gamma = 2\pi \times 10$ kHz so that $J, J' \sim 0.1\gamma$. To detect whether an atom has decayed to $|a\rangle$, one would excite $|a\rangle$ to $|P_{1/2}, F=0\rangle$ and observe the fluorescence; the absence of fluorescence means the atom has not decayed. Measuring $|a\rangle$ does not interfere with the coherent dynamics between $|\downarrow\rangle$ and $|\uparrow\rangle$, so one can measure during the experimental run; this saves time since one can just stop the run when the first atom decays.

Each run should be long enough so that the system has converged into the steady state. The timescale is estimated by $1/\Delta$, where $\Delta = \text{Im } \epsilon(\pi/2)$ is the gap. The number of decay events during this time interval is Poissonian with an average of $g \approx \gamma N(\langle\sigma_n^z\rangle + 1)/2\Delta$, so the probability of no decay events during a run is $P \approx e^{-g}$. For example, suppose $J' = J = 0.1\gamma$ and $\gamma = 2\pi \times 10$ kHz. Then each run lasts for about $50 \mu\text{s}$. For $N = 2$, $P \sim 0.3$. For $N = 20$, $P \sim 0.007$.

Conclusion.— The non-Hermitian model exhibits phases and phase transitions that are absent from the Hermitian model and master equation. Thus, non-Hermitian quantum mechanics is a promising route to find new condensed-matter phenomena. For future work,

perhaps one can map a D -dimensional non-Hermitian quantum model to a $(D+1)$ -dimensional classical model like in the Hermitian case [41]. One can also characterize the entanglement between atoms to see whether it exhibits critical behavior at the phase transition, as in the Hermitian model [51] and master equation [17]. Furthermore, it would be interesting to consider the effect of

disorder using real-space renormalization group [32].

We thank S. Sachdev, G. Refael, N. Moiseyev, S. Gopalakrishnan, and M. Foss-Feig for useful discussions. This work was supported by the NSF through a grant to ITAMP. C.K.C. is supported by the Croucher Foundation.

-
- [1] H. J. Carmichael, *An Open Systems Approach to Quantum Optics* (Springer-Verlag, Berlin, 1993).
 - [2] P. Schindler *et al.*, Nat. Phys. **9**, 361 (2013).
 - [3] E. G. D. Torre, S. Diehl, M. D. Lukin, S. Sachdev, and P. Strack, Phys. Rev. A **87**, 023831 (2013).
 - [4] L. M. Sieberer, S. D. Huber, E. Altman, and S. Diehl, Phys. Rev. Lett. **110**, 195301 (2013).
 - [5] F. Nissen, S. Schmidt, M. Biondi, G. Blatter, H. E. Türeci, and J. Keeling, Phys. Rev. Lett. **108**, 233603 (2012).
 - [6] J. Jin, D. Rossini, R. Fazio, M. Leib, and M. J. Hartmann, Phys. Rev. Lett. **110**, 163605 (2013).
 - [7] C. Carr, R. Ritter, C. G. Wade, C. S. Adams, and K. J. Weatherill, Phys. Rev. Lett. **111**, 113901 (2013).
 - [8] N. Malossi, M. Valado, S. Scotto, P. Huillery, P. Pilet, D. Ciampini, E. Arimondo, and O. Morsch, arXiv:1308.1854 (2013).
 - [9] T. E. Lee, H. Häffner, and M. C. Cross, Phys. Rev. A **84**, 031402 (2011).
 - [10] J. Qian, L. Zhou, and W. Zhang, Phys. Rev. A **87**, 063421 (2013).
 - [11] M. Foss-Feig, K. R. A. Hazzard, J. J. Bollinger, A. M. Rey, and C. W. Clark, New J. Phys. **15**, 113008 (2013).
 - [12] B. Olmos, D. Yu, and I. Lesanovsky, Phys. Rev. A **89**, 023616 (2014).
 - [13] S. Morrison and A. S. Parkins, Phys. Rev. Lett. **100**, 040403 (2008).
 - [14] T. Prosen and I. Pizorn, Phys. Rev. Lett. **101**, 105701 (2008).
 - [15] C.-E. Bardyn and A. Imamoglu, Phys. Rev. Lett. **109**, 253606 (2012).
 - [16] T. E. Lee, S. Gopalakrishnan, and M. D. Lukin, Phys. Rev. Lett. **110**, 257204 (2013).
 - [17] C. Joshi, F. Nissen, and J. Keeling, Phys. Rev. A **88**, 063835 (2013).
 - [18] M. Lemesko and H. Weimer, Nat. Commun. **4**, 2230 (2013).
 - [19] M. Hönig, M. Moos, and M. Fleischhauer, Phys. Rev. A **86**, 013606 (2012).
 - [20] B. Horstmann, J. I. Cirac, and G. Giedke, Phys. Rev. A **87**, 012108 (2013).
 - [21] J. Dalibard, Y. Castin, and K. Mølmer, Phys. Rev. Lett. **68**, 580 (1992).
 - [22] R. Dum, P. Zoller, and H. Ritsch, Phys. Rev. A **45**, 4879 (1992).
 - [23] L.-M. Duan, M. D. Lukin, J. I. Cirac, and P. Zoller, Nature **414**, 413 (2011).
 - [24] C. W. Chou, H. de Riedmatten, D. Felinto, S. V. Polyakov, S. J. van Enk, and H. J. Kimble, Nature **438**, 828 (2005).
 - [25] D. N. Matsukevich, T. Chanelière, S. D. Jenkins, S.-Y. Lan, T. A. B. Kennedy, and A. Kuzmich, Phys. Rev. Lett. **96**, 030405 (2006).
 - [26] D. L. Moehring, P. Maunz, S. Olmschenk, K. C. Younge, D. N. Matsukevich, L.-M. Duan, and C. Monroe, Nature **449**, 68 (2007).
 - [27] B. Casabone, A. Stute, K. Friebe, B. Brandstätter, K. Schüppert, R. Blatt, and T. E. Northup, Phys. Rev. Lett. **111**, 100505 (2013).
 - [28] N. Moiseyev, *Non-Hermitian Quantum Mechanics* (Cambridge University Press, 2011).
 - [29] M. V. Berry and D. H. J. O'Dell, J. Phys. A **31**, 2093 (1998).
 - [30] W. D. Heiss, J. Phys. A **45**, 444016 (2012).
 - [31] M. Liertzer, L. Ge, A. Cerjan, A. D. Stone, H. E. Türeci, and S. Rotter, Phys. Rev. Lett. **108**, 173901 (2012).
 - [32] G. Refael, W. Hofstetter, and D. R. Nelson, Phys. Rev. B **74**, 174520 (2006).
 - [33] M. S. Rudner and L. S. Levitov, Phys. Rev. Lett. **102**, 065703 (2009).
 - [34] C. M. Bender and S. Boettcher, Phys. Rev. Lett. **80**, 5243 (1998).
 - [35] G. L. Giorgi, Phys. Rev. B **82**, 052404 (2010).
 - [36] X. Z. Zhang and Z. Song, Phys. Rev. A **87**, 012114 (2013).
 - [37] J. Otterbach and M. Lemesko, arXiv:1308.5905 (2013).
 - [38] J. M. Hickey, S. Genway, I. Lesanovsky, and J. P. Garahan, Phys. Rev. B **87**, 184303 (2013).
 - [39] E. Lieb, T. Schultz, and D. Mattis, Annals of Physics **16**, 407 (1961).
 - [40] E. Barouch and B. M. McCoy, Phys. Rev. A **3**, 786 (1971).
 - [41] S. Sachdev, *Quantum Phase Transitions* (Cambridge University Press, 2007).
 - [42] A. Amir, Y. Oreg, and Y. Imry, Phys. Rev. A **77**, 050101 (2008).
 - [43] P. Werner, K. Völker, M. Troyer, and S. Chakravarty, Phys. Rev. Lett. **94**, 047201 (2005).
 - [44] K. Mølmer and A. Sørensen, Phys. Rev. Lett. **82**, 1835 (1999).
 - [45] D. Porras and J. I. Cirac, Phys. Rev. Lett. **92**, 207901 (2004).
 - [46] J. W. Britton *et al.*, Nature **484**, 489 (2012).
 - [47] R. Islam *et al.*, Science **340**, 583 (2013).
 - [48] I. Bouchoule and K. Mølmer, Phys. Rev. A **65**, 041803 (2002).
 - [49] M. Viteau, M. G. Bason, J. Radogostowicz, N. Malossi, D. Ciampini, O. Morsch, and E. Arimondo, Phys. Rev. Lett. **107**, 060402 (2011).
 - [50] L. Li, Y. O. Dudin, and A. Kuzmich, Nature **498**, 466 (2013).
 - [51] A. Osterloh, L. Amico, G. Falci, and R. Fazio, Nature **416**, 608 (2002).
 - [52] T. T. Wu, Phys. Rev. **149**, 380 (1966).

Supplemental material: Heralded magnetism in non-Hermitian atomic systems

Here, we provide more details of the Jordan-Wigner calculation for the non-Hermitian model, since there are some important differences with the Hermitian model.

Appendix A: Wick expansion

The right eigenvectors of M_k are $(u_k, v_k)^T$ and $(-v_k, u_k)^T$, where

$$u_k = \frac{i\gamma - 8J \cos k \pm 2\sqrt{(4J \cos k - i\gamma/2)^2 + (4J' \sin k)^2}}{\mathcal{C}}, \quad (\text{A1})$$

$$v_k = \frac{8J' \sin k}{\mathcal{C}}, \quad (\text{A2})$$

where the normalization constant \mathcal{C} is such that $u_k^2 + v_k^2 = 1$. The sign convention in Eq. (A1) is the same as for $\epsilon(k)$, i.e., the sign convention for each k is such that the imaginary part of $\epsilon(k)$ is negative.

The vacuum state $|G\rangle$ is defined via $\eta_k|G\rangle = 0$, and is given explicitly by

$$|G\rangle = \frac{1}{\sqrt{\mathcal{N}}} \prod_{k>0} (u_k - v_k c_k^\dagger c_{-k}^\dagger) |0\rangle, \quad (\text{A3})$$

where $\mathcal{N} = \prod_{k>0} (|u_k|^2 + |v_k|^2)$ is the normalization constant. Note that $|u_k|^2 + |v_k|^2 \neq 1$ for the non-Hermitian case. From Eq. (A3), one finds the expression for $\langle \sigma_n^z \rangle$ given in the main text.

Now we want to calculate

$$\langle \sigma_m^x \sigma_n^x \rangle = \langle B_m A_{m+1} B_{m+1} \cdots A_{n-1} B_{n-1} A_n \rangle \quad (\text{A4})$$

$$\langle \sigma_m^y \sigma_n^y \rangle = (-1)^{n-m} \langle A_m B_{m+1} A_{m+1} \cdots B_{n-1} A_{n-1} B_n \rangle \quad (\text{A5})$$

$$\langle \sigma_m^z \sigma_n^z \rangle = \langle A_m B_m A_n B_n \rangle \quad (\text{A6})$$

for $|G\rangle$, where $A_n = c_n^\dagger + c_n$ and $B_n = c_n^\dagger - c_n$. To calculate these, we use Wick's theorem. However, when applying Wick's theorem, it is convenient use η_k, η_k^\dagger instead of $\eta_k, \bar{\eta}_k$, since $\langle G | \eta_k^\dagger = 0$ while $\langle G | \bar{\eta}_k \neq 0$. So we note that

$$\tilde{c}_k = \frac{u_k^* \eta_k - v_k \eta_{-k}^\dagger}{|u_k|^2 + |v_k|^2}, \quad \tilde{c}_{-k} = \frac{u_k^* \eta_{-k} + v_k \eta_k^\dagger}{|u_k|^2 + |v_k|^2}, \quad (\text{A7})$$

and $\langle \eta_k \eta_k^\dagger \rangle = |u_k|^2 + |v_k|^2$. Then we do a Wick expansion of Eqs. (A4)–(A6) in terms contractions of operator pairs. For example,

$$\langle \sigma_m^z \sigma_n^z \rangle = \langle A_m B_m \rangle \langle A_n B_n \rangle - \langle A_m B_n \rangle \langle A_n B_m \rangle - \langle A_m A_n \rangle \langle B_m B_n \rangle \quad (\text{A8})$$

$$= \langle \sigma_m^z \rangle \langle \sigma_n^z \rangle - \langle A_m B_n \rangle \langle A_n B_m \rangle - \langle A_m A_n \rangle \langle B_m B_n \rangle. \quad (\text{A9})$$

The pair contractions for A_n and B_n are

$$\langle A_m A_n \rangle = \delta_{mn} + \frac{1}{\pi} \int_0^\pi dk \sin k(n-m) \left(\frac{u_k v_k^* - u_k^* v_k}{|u_k|^2 + |v_k|^2} \right), \quad (\text{A10})$$

$$\langle B_m B_n \rangle = -\delta_{mn} + \frac{1}{\pi} \int_0^\pi dk \sin k(n-m) \left(\frac{u_k v_k^* - u_k^* v_k}{|u_k|^2 + |v_k|^2} \right), \quad (\text{A11})$$

$$\langle B_m A_n \rangle = -\langle A_n B_m \rangle \quad (\text{A12})$$

$$= -\frac{1}{\pi} \int_0^\pi dk \cos k(n-m) \left(\frac{|u_k|^2 - |v_k|^2}{|u_k|^2 + |v_k|^2} \right) + \frac{1}{\pi} \int_0^\pi dk \sin k(n-m) \left(\frac{u_k v_k^* + u_k^* v_k}{|u_k|^2 + |v_k|^2} \right). \quad (\text{A13})$$

These expressions are different from the Hermitian case [39]. In particular, $\langle A_m A_n \rangle$ and $\langle B_m B_n \rangle$ can be nonzero even when $m \neq n$. (This prevents us from writing $\langle \sigma_m^x \sigma_n^x \rangle$ in terms of a Toeplitz determinant and using Szegő's theorem [40, 41].)

Since $\langle \sigma_m^x \sigma_n^x \rangle$ and $\langle \sigma_m^y \sigma_n^y \rangle$ may contain many operators, it is useful to write them in terms of the Pfaffian of a skew-symmetric matrix [40]:

$$\langle \sigma_m^x \sigma_n^x \rangle = \text{pf} \begin{pmatrix} 0 & \langle B_m B_{m+1} \rangle & \langle B_m B_{m+2} \rangle & \cdots & \langle B_m B_{n-1} \rangle & \langle B_m A_{m+1} \rangle & \langle B_m A_{m+2} \rangle & \cdots & \langle B_m A_n \rangle \\ & 0 & \langle B_{m+1} B_{m+2} \rangle & \cdots & \langle B_{m+1} B_{n-1} \rangle & \langle B_{m+1} A_{m+1} \rangle & \langle B_{m+1} A_{m+2} \rangle & \cdots & \langle B_{m+1} A_n \rangle \\ & & 0 & \cdots & \vdots & \vdots & \vdots & \vdots & \vdots \\ & & & \langle B_{n-2} B_{n-1} \rangle & \langle B_{n-2} A_{m+1} \rangle & \langle B_{n-2} A_{m+2} \rangle & \cdots & \langle B_{n-2} A_n \rangle \\ & & & 0 & \langle B_{n-1} A_{m+1} \rangle & \langle B_{n-1} A_{m+2} \rangle & \cdots & \langle B_{n-1} A_n \rangle \\ & & & & 0 & \langle A_{m+1} A_{m+2} \rangle & \cdots & \langle A_{m+1} A_n \rangle \\ & & & & & \cdots & \vdots & \vdots \\ & & & & & & \langle A_{n-1} A_n \rangle & 0 \end{pmatrix}, \quad (\text{A14})$$

and similarly for $\langle \sigma_m^y \sigma_n^y \rangle$. The elements on the bottom left are given by the skew-symmetry. This matrix has dimensions $2|m-n| \times 2|m-n|$. The Pfaffian of a matrix can be efficiently computed using the fact that $\text{pf}(D)^2 = \det(D)$, but this method does not give the sign of the Pfaffian. If one needs the sign of $\langle \sigma_m^x \sigma_n^x \rangle$, it is necessary to explicitly calculate the Wick expansion, which is computationally slower.

Appendix B: Asymptotic behavior of the correlation function

In this section, we compute the z -component correlation function

$$\begin{aligned} C^{zz}(x) &= \langle \sigma_0^z \sigma_x^z \rangle - \langle \sigma_0^z \rangle \langle \sigma_x^z \rangle \\ &= -\langle A_0 B_x \rangle \langle A_x B_0 \rangle - \langle A_0 A_x \rangle \langle B_0 B_x \rangle \end{aligned} \quad (\text{B1})$$

for long distances. The goal is to calculate the critical exponent ν , which describes the divergence of the correlation length as $|J'|$ increases toward $\gamma/8$. We consider the cases of $J = 0$ and $J \neq 0$ separately.

1. Case of $J = 0$

In this case, the sign conventions of ϵ_k and u_k are independent of k . When $|x| > 1$, we have $\langle A_0 A_x \rangle = \langle B_0 B_x \rangle = 0$ and $C^{zz}(x) = -\langle B_0 A_x \rangle^2$, where

$$\langle B_0 A_x \rangle = -\frac{1}{\pi} \int_0^\pi dk \cos kx \sqrt{1 - \left(\frac{8J'}{\gamma} \right)^2 \sin^2 k}, \quad (\text{B2})$$

which is non-zero only for even x . We follow the procedure introduced in Ref. [52] to evaluate the integral above in the limit $x \rightarrow \infty$. We first transform Eq. (B2) into a contour integral by a change of variable, $z = ie^{ik}$, so that

$$\langle B_0 A_x \rangle = \frac{2i^x |J'|}{\pi \gamma} \oint dz z^{x-1} \sqrt{\frac{(z^2 - z_1^2)(z^2 - z_2^2)}{z^2}}, \quad (\text{B3})$$

where the contour is along the unit circle. The roots of the polynomial $z^4 + [2 - \gamma^2/(16J'^2)]z^2 + 1$, denoted by $\pm z_1$ and $\pm z_2$ with $|z_1| < 1 < |z_2|$, lie on the real axis. We then deform the contour to be along the real axis and further make a change of variable, $y = z/z_1$, to obtain the expression:

$$\langle B_0 A_x \rangle = -\frac{8i|J'|}{\pi \gamma} (iz_1)^{x+1} \int_0^1 dy y^{x-2} \sqrt{(y^2 - 1) \left[y^2 - \left(\frac{z_2}{z_1} \right)^2 \right]}. \quad (\text{B4})$$

Now, in the large x limit, the integrand is dominated by $y = 1$, so we expand the square root around $y = 1$ to get:

$$\begin{aligned}
\langle B_0 A_x \rangle &\doteq -\frac{8i|J'|}{\pi\gamma}(iz_1)^{x+1} \sum_{n=0} \frac{(-1)^{n+1}(2n-3)!!}{2^n n!} \left[\left(\frac{z_2}{z_1} \right)^2 - 1 \right]^{\frac{1-2n}{2}} \times \int_0^1 dy y^{x-2} (1-y^2)^{\frac{2n+1}{2}} \\
&= -\frac{4i|J'|}{\pi\gamma}(iz_1)^{x+1} \sum_{n=0} \frac{(-1)^{n+1}(2n-3)!!}{2^n n!} \frac{\Gamma(n+\frac{3}{2})\Gamma(\frac{x-1}{2})}{\Gamma(\frac{x}{2}+n+1)} \left[\left(\frac{z_2}{z_1} \right)^2 - 1 \right]^{\frac{1-2n}{2}} \\
&= -4i\sqrt{\frac{2}{\pi}} \frac{|J'|}{\gamma} (iz_1)^{x+1} x^{-\frac{3}{2}} \left[\left(\frac{z_2}{z_1} \right)^2 - 1 \right]^{\frac{1}{2}} \left\{ 1 + \frac{3}{2x} \left[\left(\frac{z_2}{z_1} \right)^2 - 1 \right]^{-1} + \mathcal{O}\left(\frac{1}{x^2}\right) \right\}, \tag{B5}
\end{aligned}$$

where \doteq means that the two expressions are asymptotically the same. Therefore, the z -component correlation has the following asymptotic behavior for even x :

$$C^{zz}(x \gg 1) \doteq -\frac{32}{\pi} \left(\frac{J'}{\gamma} \right)^2 x^{-3} z_1^{2x+2} \times \left[\left(\frac{z_2}{z_1} \right)^2 - 1 + \frac{3}{x} + \mathcal{O}\left(\frac{1}{x^2}\right) \right], \tag{B6}$$

or $C^{zz}(x) \sim x^{-3} e^{-x/\xi}$ with $\xi = -1/(2 \ln z_1)$. Near the critical point,

$$\xi = \frac{1}{8(\frac{1}{8} - \frac{|J'|}{\gamma})^{\frac{1}{2}}}, \tag{B7}$$

so the critical exponent ν is $1/2$.

2. Case of $J \neq 0$

The asymptotic behavior for the $J \neq 0$ case can be carried out in a similar manner. We shall consider only even x . For $|x| > 1$, we find:

$$\langle B_0 A_{\pm x} \rangle = \text{Re} \left\{ -\frac{\text{sgn}(J)}{\pi} \int_{-\frac{\pi}{2}}^{\frac{\pi}{2}} dk \left[-i \cos kx \pm \sin kx \left(\frac{-1 + 8iJ \cos k/\gamma}{8J' \sin k/\gamma} \right) \right] \sqrt{(i - 8J \cos k/\gamma)^2 + (8J' \sin k/\gamma)^2} \right\}, \tag{B8}$$

where $\text{sgn}(J)$ is the sign of J , $\langle A_0 A_x \rangle = \langle B_0 B_x \rangle = 0$ and $\langle A_0 B_x \rangle = -\langle B_0 A_{-x} \rangle$. We convert the integral into a contour integral using $\tilde{z} = ie^{ik}$ again and obtain

$$\langle B_0 A_{\pm x} \rangle = \text{Re} \left\{ \frac{i^x \text{sgn}(J)}{\pi} \oint d\tilde{z} \tilde{z}^{|x|-1} \left[\frac{4(J' \mp J) \pm \frac{8J/\gamma + \tilde{z}}{1+\tilde{z}^2} \gamma}{4J'} \right] \tilde{F}(\tilde{z})^{1/2} \right\}, \tag{B9}$$

$$\tilde{F}(\tilde{z}) = \frac{16(J'^2 - J^2)}{\gamma^2} \tilde{z}^2 - \frac{8J}{\gamma} \tilde{z} + \left[\frac{32(J'^2 + J^2)}{\gamma^2} - 1 \right] + \frac{8J}{\gamma} \tilde{z}^{-1} + \frac{16(J'^2 - J^2)}{\gamma^2} \tilde{z}^{-2}, \tag{B10}$$

where the contour is along the upper arc of the unit circle in the counter-clockwise sense. Similar to the $J = 0$ case, we deform the contour along the branch cut defined by the roots of $\tilde{F}(\tilde{z}) = 0$ and the origin. There are 4 and 2 real roots when $|J'| \neq |J|$ and $|J'| = |J|$, respectively. The correlation length is determined by the largest root with $|\tilde{z}_L| < 1$ through $\xi = -1/(2 \ln |\tilde{z}_L|)$. Solving Eq. (B10) near the critical point, we get $|\tilde{z}_L| \approx 1 - (1/8 - |J'|/\gamma)\gamma/|J|$. Therefore, for $J \neq 0$, we have

$$\xi = \frac{|J|}{2\gamma(\frac{1}{8} - \frac{|J'|}{\gamma})}, \tag{B11}$$

so $\nu = 1$.

Following the same procedure, the asymptotic behavior of the z -component correlation can be evaluated in a lengthy but straightforward way by expanding Eq. (B9). The result for $|x| \gg 1$ is summarized here:

$$C^{zz}(|x|) = \begin{cases} \frac{4(J^2 - J'^2)}{\pi} |x|^{-3} \left\{ \left[\sum_{i=1,2} \tilde{z}_i^{|x|} \left(g_{i,0}^+ + \frac{3g_{i,1}^+}{2|x|} \right) \right] \left[\sum_{i=1,2} \tilde{z}_i^{|x|} \left(g_{i,0}^- + \frac{3g_{i,1}^-}{2|x|} \right) \right] + \mathcal{O}\left(\frac{1}{x^2}\right) \right\}, & |J'| > |J| \\ \frac{4(J'^2 - J^2)}{\pi} \tilde{z}_2^{2|x|} |x|^{-3} \left[\left(g_{2,0}^+ + \frac{3g_{2,1}^+}{2|x|} \right) \left(g_{2,0}^- + \frac{3g_{2,1}^-}{2|x|} \right) + \mathcal{O}\left(\frac{1}{x^2}\right) \right], & |J'| < |J| \\ \frac{2J}{\pi} \tilde{z}_1^{2|x|} |x|^{-3} \left[\left(g_{1,0}^+ + \frac{3g_{1,1}^+}{2|x|} \right) \left(g_{1,0}^- + \frac{3g_{1,1}^-}{2|x|} \right) + \mathcal{O}\left(\frac{1}{x^2}\right) \right], & |J'| = |J| \end{cases} \quad (\text{B12})$$

where the coefficients $g_{i,n}^\pm$ are obtained from the expansion:

$$G^\pm(\tilde{z}_i y) = \sum_{n=0} g_{i,n}^\pm (1-y)^{\frac{2n+1}{2}},$$

$$G^\pm(\tilde{z}) = \begin{cases} \left[\frac{4(J' \mp J) \pm \frac{8J/\gamma + \tilde{z}}{1 + \tilde{z}^2} \gamma}{4J'} \right] \sqrt{\frac{(\tilde{z} - \tilde{z}_1)(\tilde{z} - \tilde{z}_2)(\tilde{z} - \tilde{z}_3)(\tilde{z} - \tilde{z}_4)}{\tilde{z}^2}}, & |J'| \neq |J| \\ \left[\frac{4(J' \mp J) \pm \frac{8J/\gamma + \tilde{z}}{1 + \tilde{z}^2} \gamma}{4J'} \right] \sqrt{\frac{(\tilde{z} - \tilde{z}_1)(\tilde{z} - \tilde{z}_2)}{\tilde{z}}}, & |J'| = |J| \end{cases} \quad (\text{B13})$$

The roots of Eq. (B10) are labeled such that $|\tilde{z}_1| < |\tilde{z}_2| < 1 < |\tilde{z}_3| < |\tilde{z}_4|$ when $|J'| \neq |J|$, and $|\tilde{z}_1| < 1 < |\tilde{z}_2|$ when $|J'| = |J|$.